Hard x-ray diffraction imaging at modern synchrotrons and free electron lasers:

the role of iterative phase retrieval methods

Daniele Pelliccia

School of Physics – Monash University
daniele.pelliccia@monash.edu

MONASH University

Monash University - Melbourne

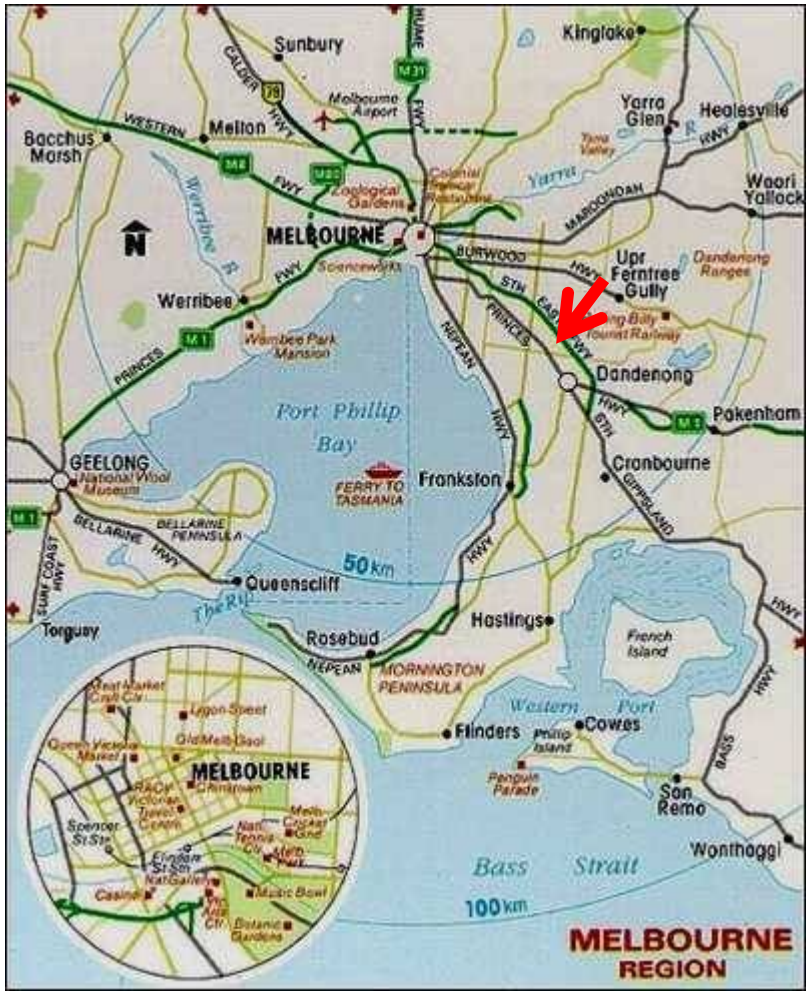

Monash University precinct

Australian Synchrotron

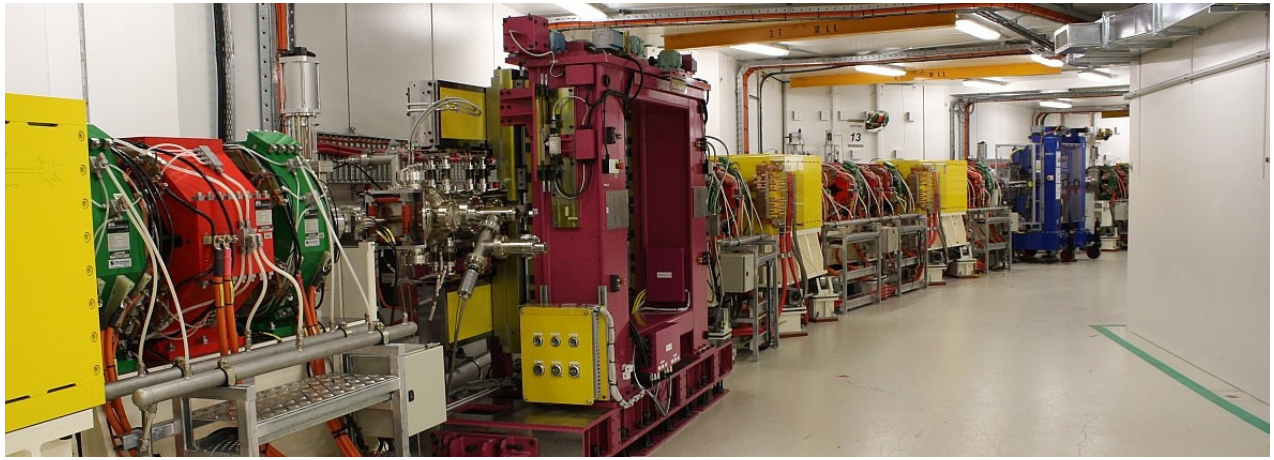

Specifications

Energy	3 GeV
Total design current	200 mA
Circumference	216 metres
RF frequency	499.654 ± 0.1 MHz
Energy loss per turn (dipoles only)	931 keV
Dipole field (nominal)	1.3 T
Beam size in dipoles	σ_x – 87μm, σ_y – 60μm
Beam size in straights	σ_x – 320μm, σ_y – 16μm
Number of possible Insertion devices	12
Emittance	ε_x – 10 nm
Coupling (nominal)	1%

http://www.synchrotron.org.au/images/newsEventsPublications/Publications/Machine-fact-sheet_23Oct08_final.pdf

Australian Synchrotron cont.

MONASH University

8 beamline currently in operation

- IR spectroscopy
- Soft x-rays spectromicroscopy
- Hard x-rays absorption and scattering beamlines
- Hard x-ray imaging for medical research and therapy (open 2013)

Techniques available at the Australian Synchrotron

Beamline	Techniques	Capabilities
Imaging and medical therapy	Phase contrast enhanced high energy x-ray imaging	Very flexible beamline for research into high contrast imaging of objects from small animals through to engineering components. For research into the physics and biophysics of cancer therapy techniques.
Infrared spectroscopy (including high spectral resolution far-IR)	Fourier Transform infrared spectroscopy and infrared microspectroscopy	Analysis of bond structures in complex molecules, biological materials, minerals and band structures in certain semi-conductors.
Microspectroscopy (x-ray fluorescence microprobe)	X-ray absorption and emission spectroscopy at a submicron scale	For producing high-resolution maps of elemental distribution in a sample with very low detection limits (μg/g). Also for determining the oxidation state and coordination geometry of atoms in samples, down to 100nm size.
Powder diffraction	Medium to high energy powder x-ray diffraction	Versatile high resolution powder diffraction facility equipped with sample holders for a wide range of in-situ experiments.
Protein crystallography, high-throughput	Medium energy, multiple wavelength anomalous dispersion x-ray diffraction	Dedicated facility for crystallography of protein crystals, set up with robotic loading and centring, and for remote operation.
Protein microcrystal and small molecule diffraction	Medium energy, multiple wavelength anomalous dispersion x-ray diffraction	Facility with finely focussed x-ray beam for determining the crystal structure and electron density maps of small, hard–to-crystallise proteins, nucleic acids and for small molecules.
Small angle and wide angle x-ray scattering	Medium energy small angle x-ray scattering/wide angle x-ray scattering	Measurement of atomic and nano-scale structure in complex molecules and materials.
Soft x-ray spectroscopy	Low energy x-ray absorption and emission spectroscopy	Measurement of short and medium range order, bond lengths, coordination numbers and local coordination geometry, and the oxidation state of atoms for the light elements, Z<20. Also for the analysis of surfaces and thin films.
X-ray absorption spectroscopy	Medium and high energy x-ray absorption and emission spectroscopy	As for soft x-ray spectroscopy, from atomic number Z=20 upwards.

http://www.synchrotron.org.au/images/newsEventsPublications/Publications/AS-factsheet-blue-final.pdf

Synopsis

1. Development of brilliance and coherence in hard x-ray sources
2. The role of x-ray crystallography
3. The phase problem in crystallography and imaging: phase retrieval
4. Iterative retrieval of the longitudinal charge distribution of an electron bunch

Science
AAAS

Natively Inhibited *Trypanosoma brucei* Cathepsin B Structure Determined by Using an X-ray Laser

Lars Redecke *et al.*

Science **339**, 227 (2013);
DOI: 10.1126/science.1229663

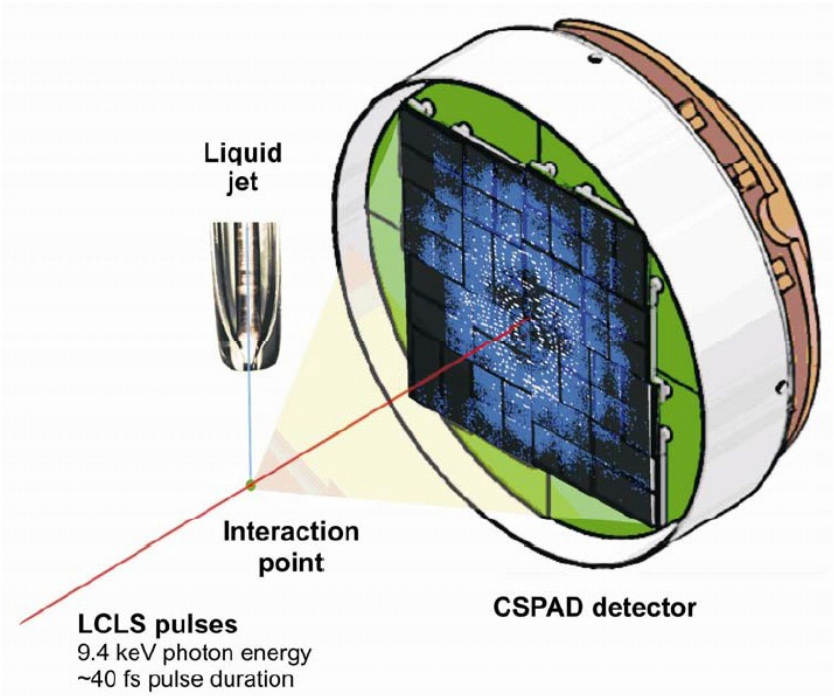

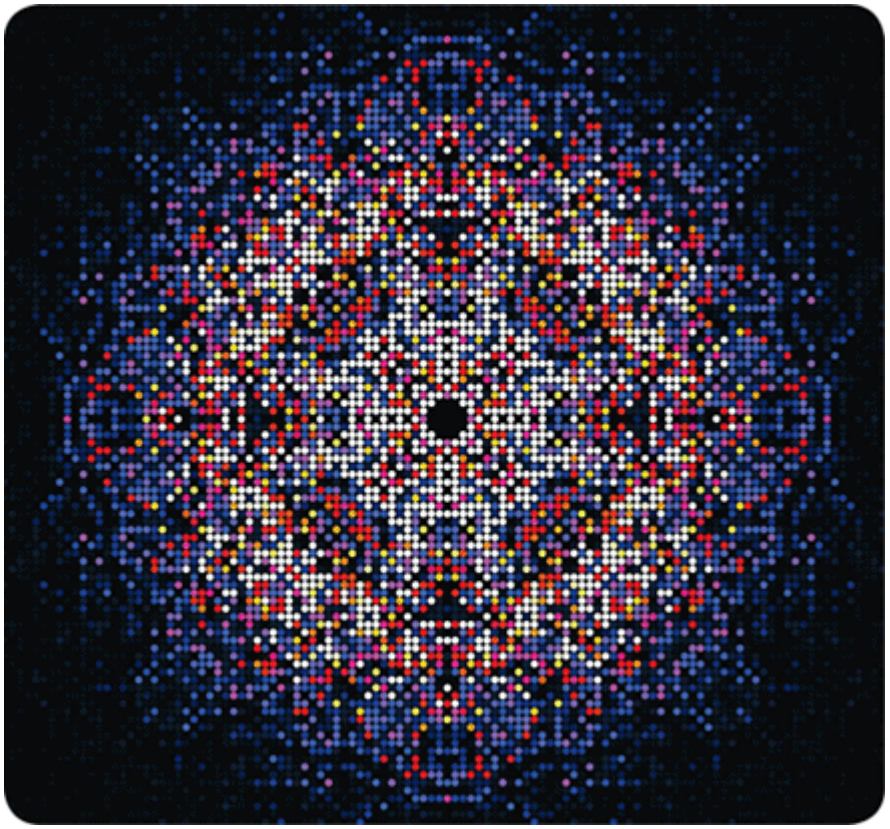

Evolution of brilliance for x-ray sources

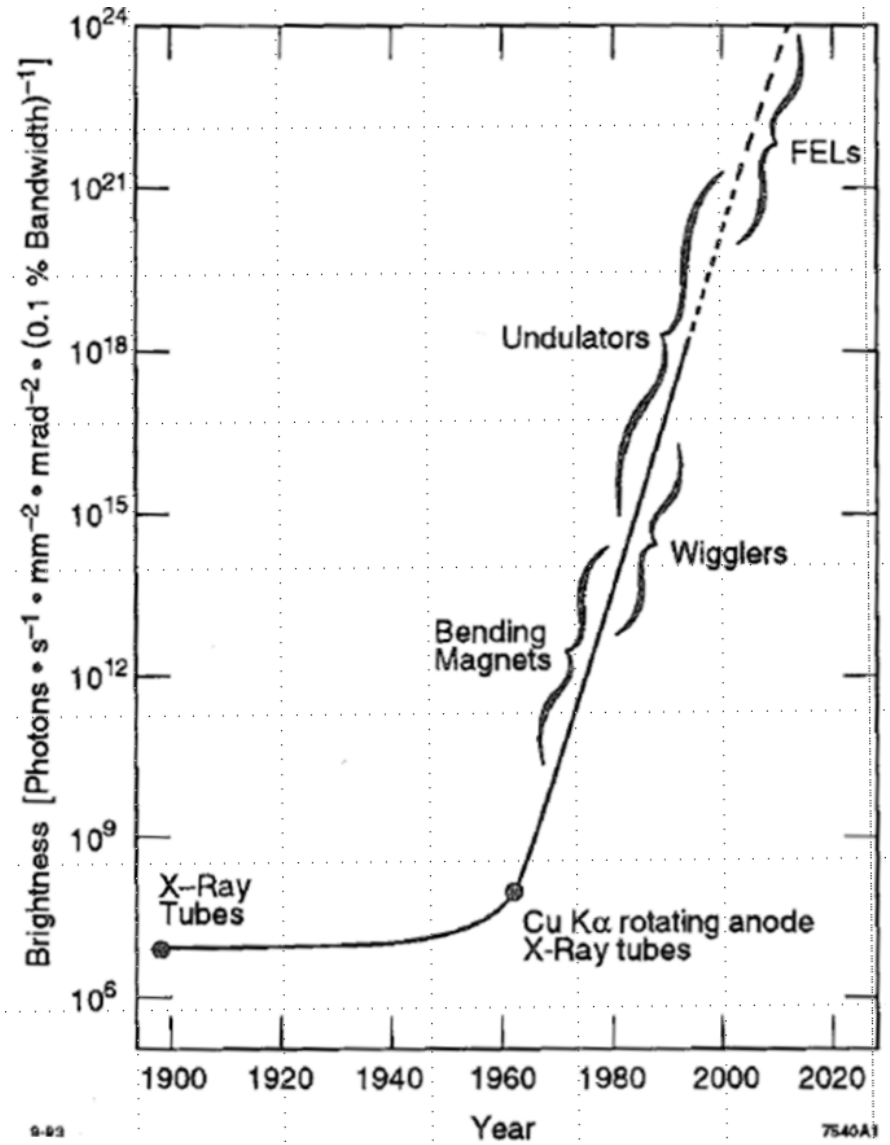

H. Winick ed,
Synchrotron Radiation Sources: A primer

Brilliance and coherence

$$Br = \frac{\text{photons}}{\text{sec mrad}^2 \text{ mm}^2 \text{ BW}0.1\%}$$

The number of photon in a mode (coherence volume) is proportional to the brilliance

$$N_c \approx \frac{\lambda_0^3}{c} Br$$

Source	Power	Brilliance	N_c
Hg lamp	1 W	$2\ 10^{11}$	0.003
ESRF undulator @ 6 keV	~ kW	$2\ 10^{20}$	0.002
He-Ne laser	1mW	$8\ 10^{19}$	2×10^{7}
XFEL @ 6 keV	10 GW	$\sim 10^{26}$	$\sim 10^{9}$
ILL 25 meV neutrons	$2\ 10^{15}$ neutrons/sec	500	3×10^{-15}

Brilliance and focusing

The Race to X-ray Microbeam and Nanobeam Science
Gene E. Ice *et al.*
Science **334**, 1234 (2011);
DOI: 10.1126/science.1202366

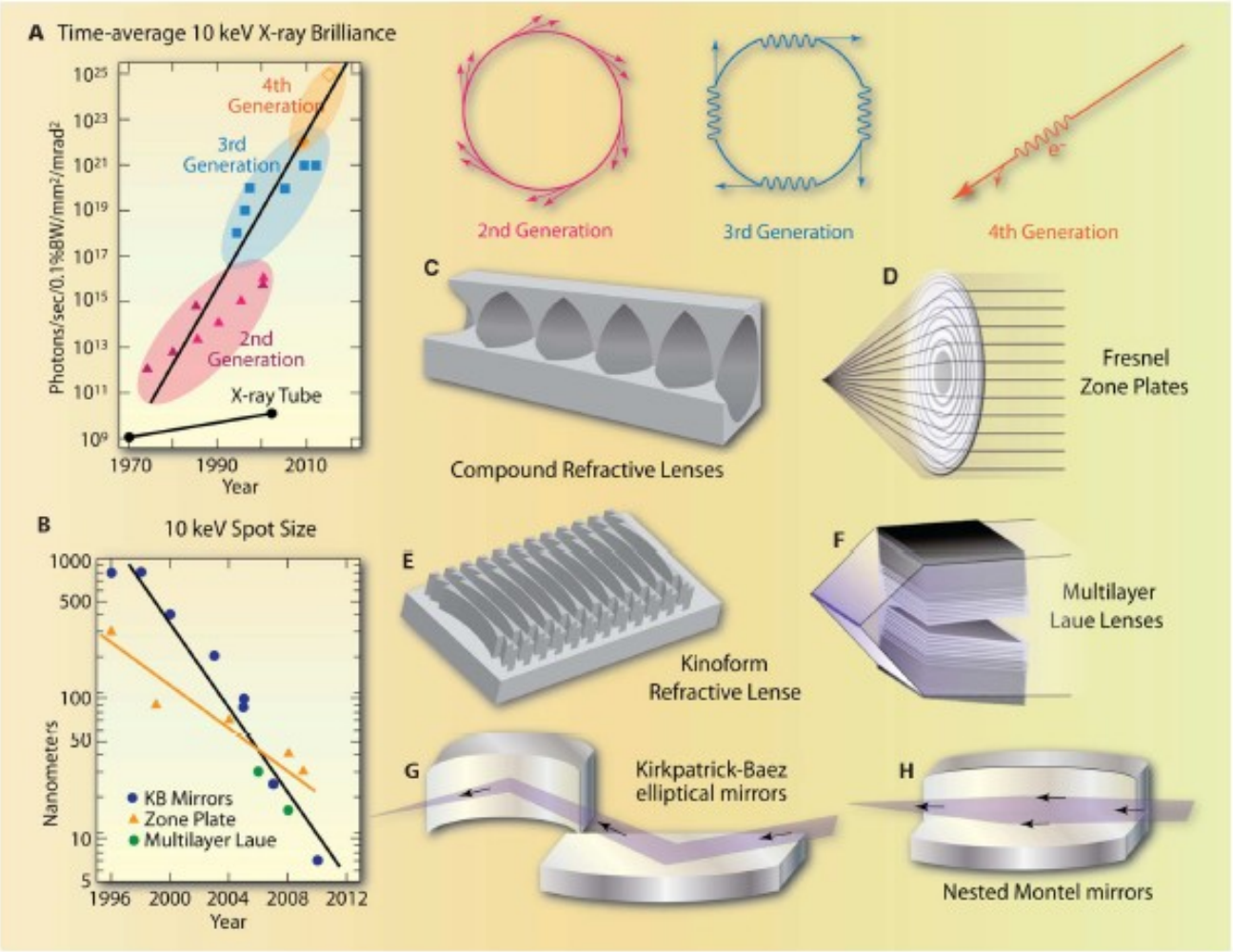

Higher brilliance enables focusing at ~10 nm level

1. Development of brilliance and coherence in hard x-ray sources
2. The role of x-ray crystallography
3. The phase problem in crystallography and imaging: phase retrieval
4. Iterative retrieval of the longitudinal charge distribution of an electron bunch

Why x-ray crystallography

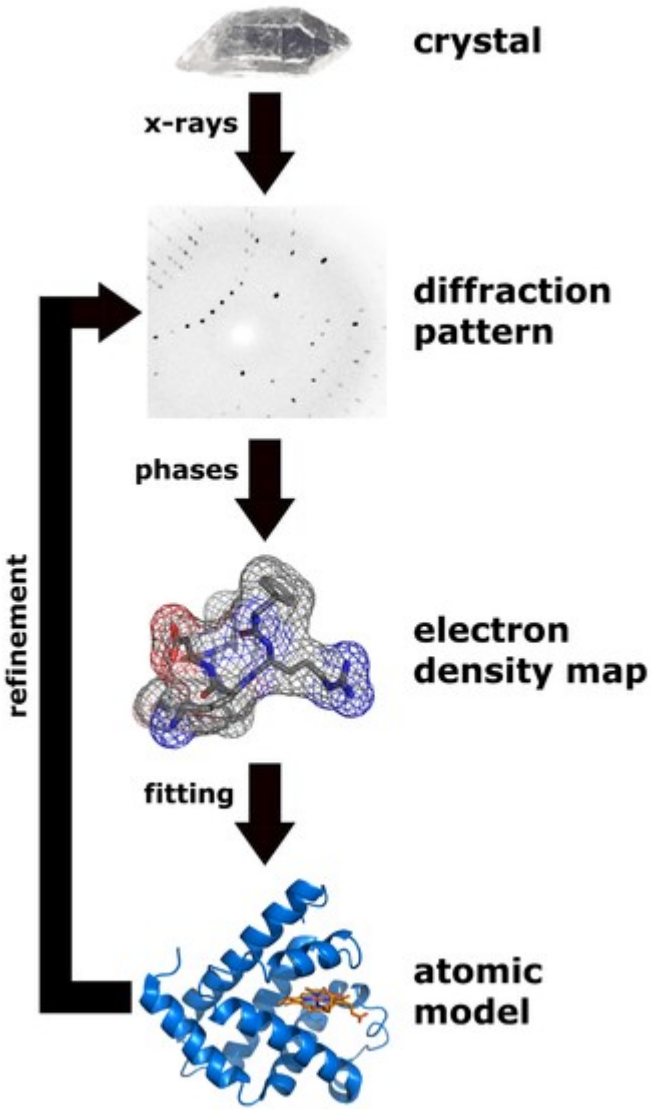

http://en.wikipedia.org/wiki/File:X_ray_diffraction.png

Why use x-rays....

Pros:
- Non-destructive
- Access the bulk
-Natural contrast for bio-samples

Cons:
- Weak interaction
- Imaging resolution (~ optical, << TEM)
- Radiation damage

X-ray crystallography overcomes many of these limitations...

- Diffraction from each cell sums up coherently into intense Bragg peaks
- Radiation damage is spread over ~10^{10} unit cells

... but it needs crystals

Synchrotron radiation and crystallography

Proc. Nat. Acad. Sci. USA
Vol. 73, No. 1, pp. 128–132, January 1976
Biophysics

Applications of synchrotron radiation to protein crystallography: Preliminary results

ABSTRACT X-ray diffraction photographs of protein single crystals have been obtained using synchrotron radiation produced by an electron-positron storage ring.

Diffraction data have been collected by the precession method to higher resolution and using smaller protein crystals than would have been possible with a conventional source. The crystal decay rate in the synchrotron beam for several proteins appears to be substantially less than that observed with Ni-filtered Cu radiation. The tunable nature of the source (which allows selective optimization of anomalous contributions to the scattering factors) and the low angular divergence of the beam make the source very useful for single crystal protein diffraction studies.

Data from SPEAR electron-positron storage ring at SLAC

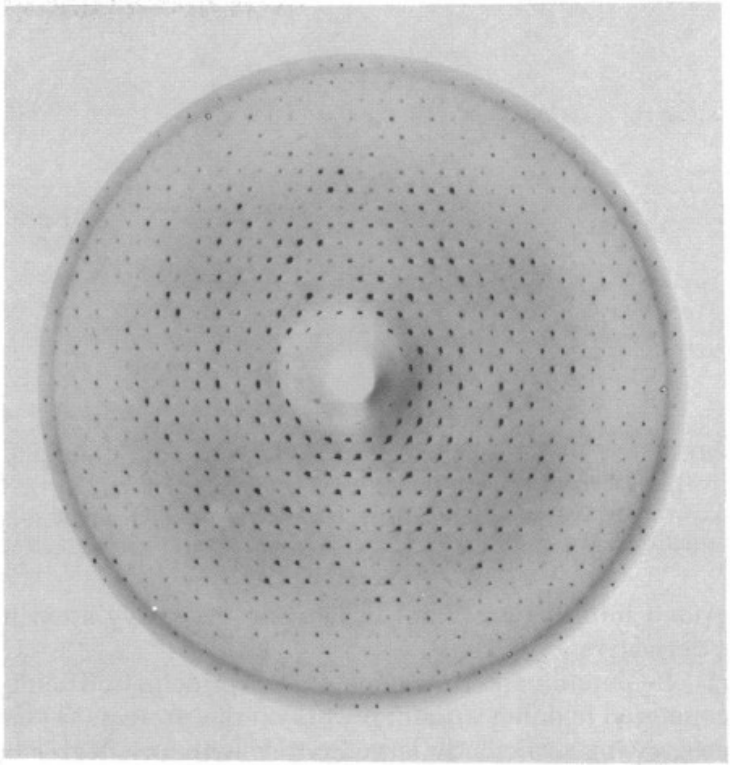

FIG. 1. Precession photograph of the *hkO* plane of a rubredoxin crystal. Synchrotron radiation, E = 3.7 GeV, average current 19 mA, λ = 1.744 Å, precession angle μ = 25°, exposure time 5 hr.

Protein structures solved with synchrotron radiation

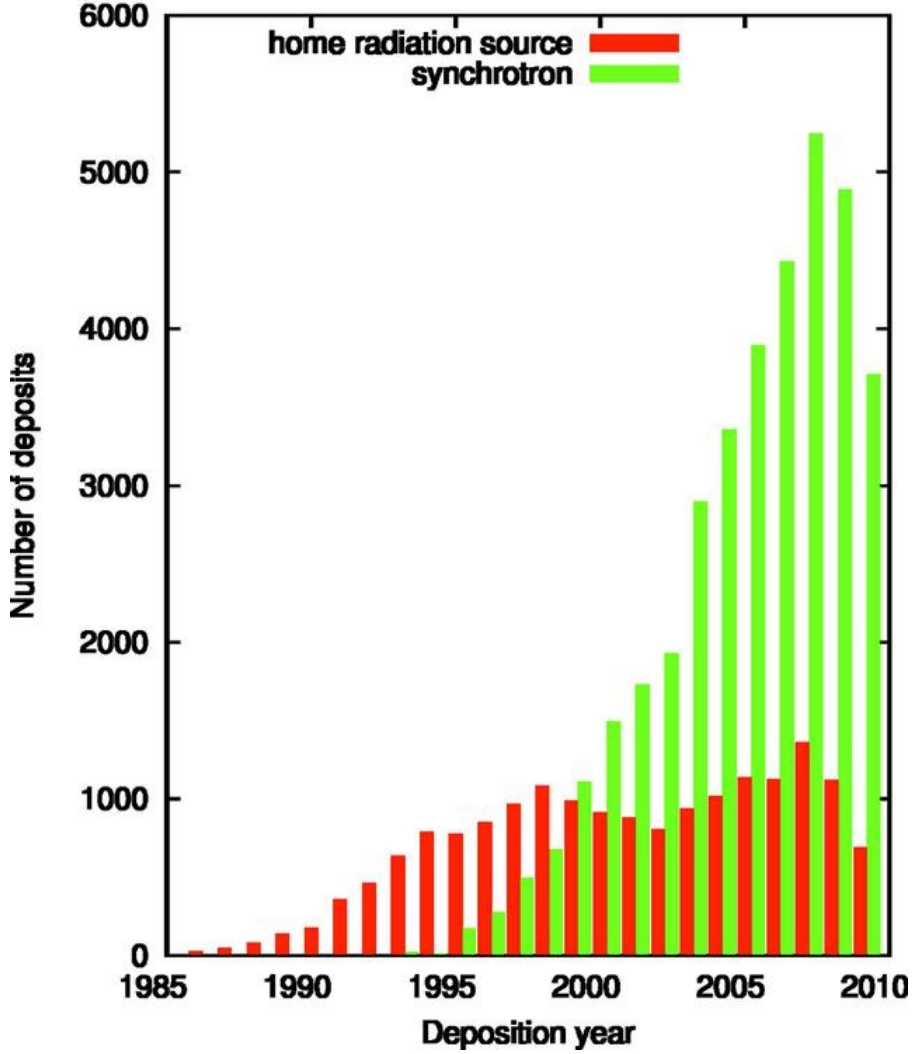

Dauter, Jaskolski, Wlodawer, J. Synchrotron Rad. **17**, 433 (2010)

The number of structures deposited annually in the Protein Data Bank. Structures determined with the use of synchrotron radiation are represented in green, and those with conventional sources in red. The data represent the time window between 1985 and 2009, (2009 statistics still incomplete)

Protein and membrane protein

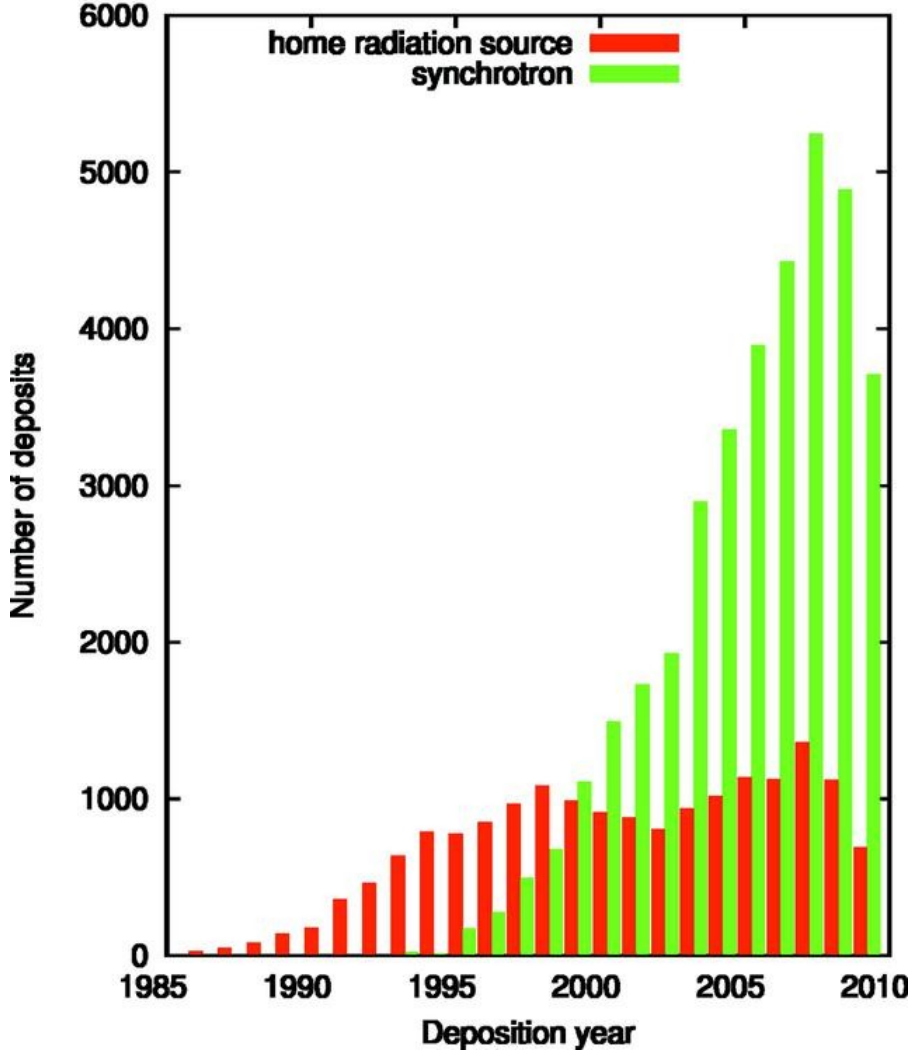

Dauter, Jaskolski, Wlodawer, J. Synchrotron Rad. **17**, 433 (2010)

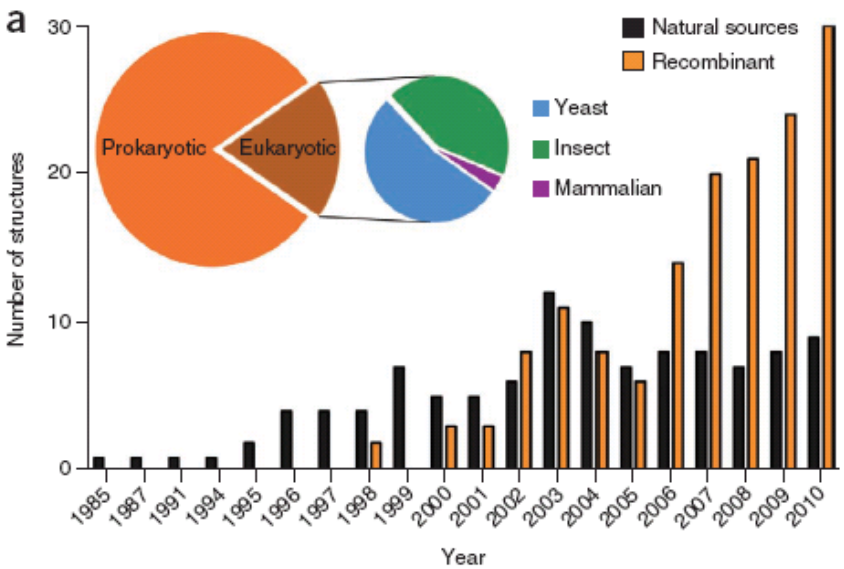

After decades of slow progress, the pace of research on membrane protein structures is beginning to quicken thanks to various improvements in technology, including protein engineering and microfocus X-ray diffraction. Here we review these developments and, where possible, highlight generic new approaches to solving membrane protein structures based on recent technological advances.

R.M. Bill et al, Nature Biotech **29**, 335 (2011)

X-ray crystallography with Free electron lasers

Membrane proteins are hard to pack into 3D crystals of sufficient size.

Science AAAS

Natively Inhibited *Trypanosoma brucei* Cathepsin B Structure Determined by Using an X-ray Laser
Lars Redecke *et al.*
Science **339**, 227 (2013);
DOI: 10.1126/science.1229663

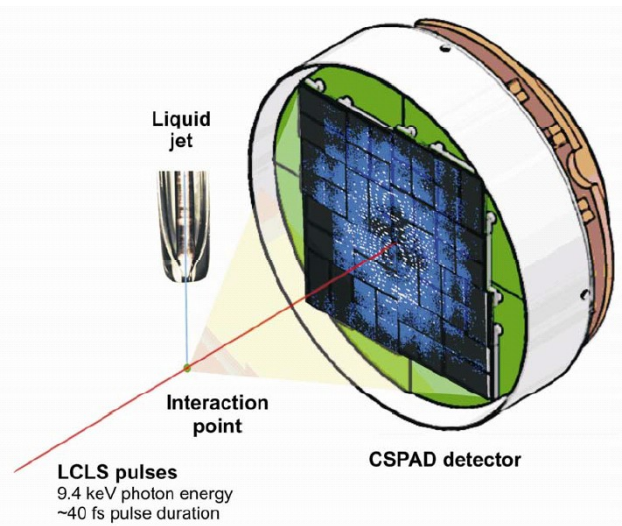

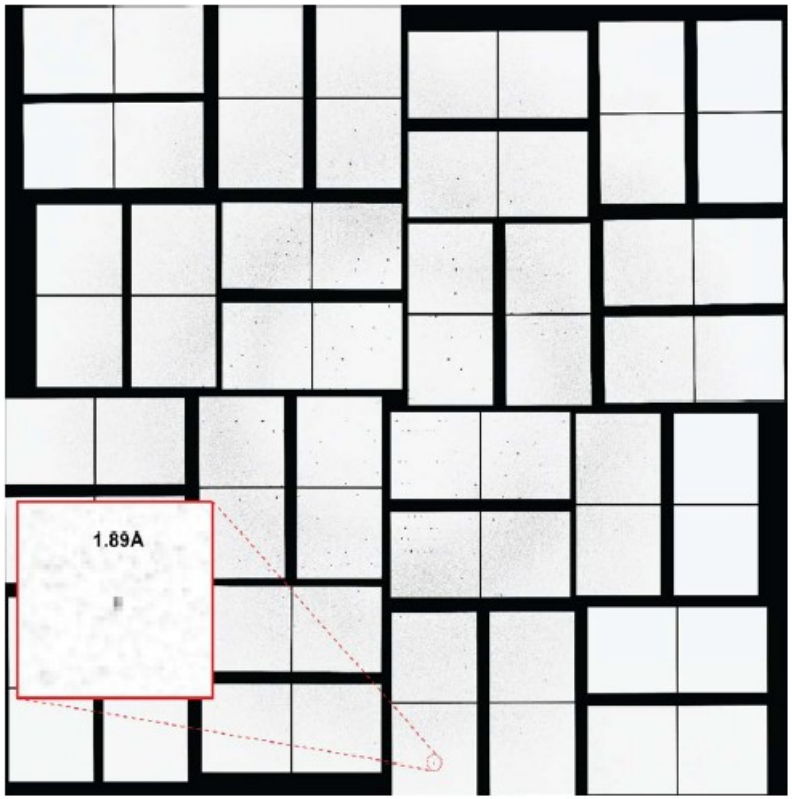

X-ray lasers can make images using micro-crystals, possibly single molecules thanks to the high brilliance

1. Development of brilliance and coherence in hard x-ray sources
2. The role of x-ray crystallography
3. **The phase problem in crystallography and imaging: phase retrieval**
4. Iterative retrieval of the longitudinal charge distribution of an electron bunch

The phase problem

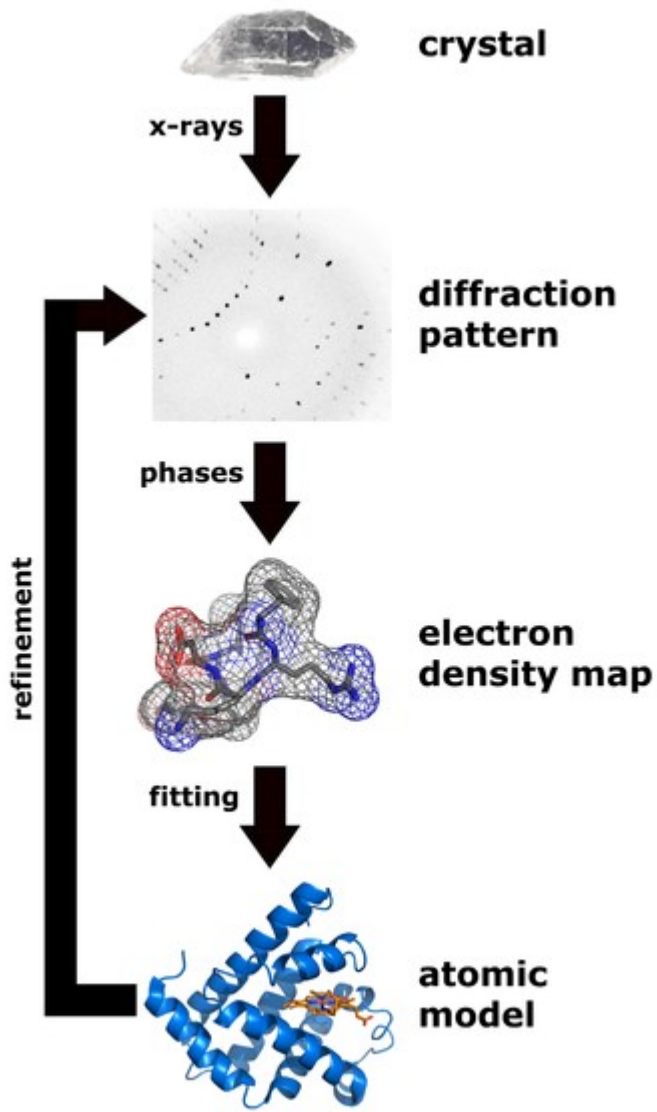

There is a Fourier transform relation between the electron density of a sample and the amplitude of the diffracted field

$$F(\mathbf{q}) = \int_{-\infty}^{\infty} \rho(\mathbf{r}) e^{-2\pi i \mathbf{q}\cdot\mathbf{r}} \mathrm{d}\mathbf{r}$$

While only the intensity is measured....

$$I(\mathbf{q}) \propto |F(\mathbf{q})|^2$$

The phase is unknown!

Phase information is lost in the detection and must be recovered to solve the structure.

http://en.wikipedia.org/wiki/File:X_ray_diffraction.png

Coherent diffractive imaging

D. Sayre (1980) proposed a "crystallographic" approach to image non-periodic objects with soft x-rays.

The far-field diffracted amplitude from a (non-periodic) sample obtained with coherent is the Fourier transform of the sample electron density.

This approach can potentially overcome the resolution limitation due to the small NA of x-ray optics.

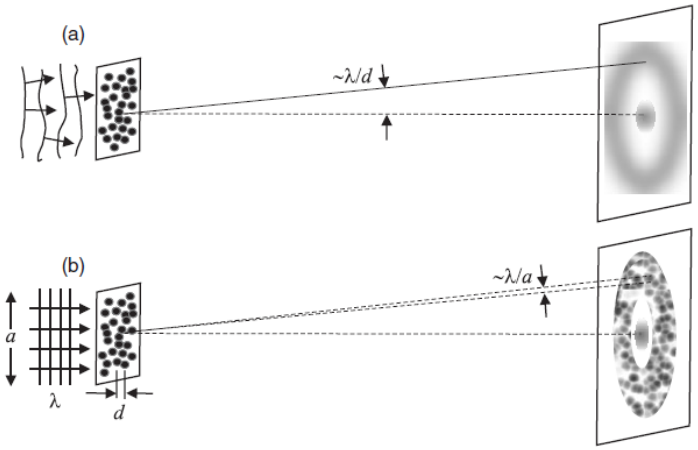

Figure 6. X-ray diffraction from a disordered medium with particle distance d. The object size is a. (a) Incoherent scattering, giving rise to a continuous diffraction ring; (b) coherent scattering, resulting in a speckled diffraction ring.

$$\text{Resolution} \sim \frac{\lambda}{\sin\theta}$$

We still need the phase though....

F. Van der Veen and F. Pfeiffer, J. Phys. Condens. Matter **16**, 5003 (2004)

Phase retrieval algorithms

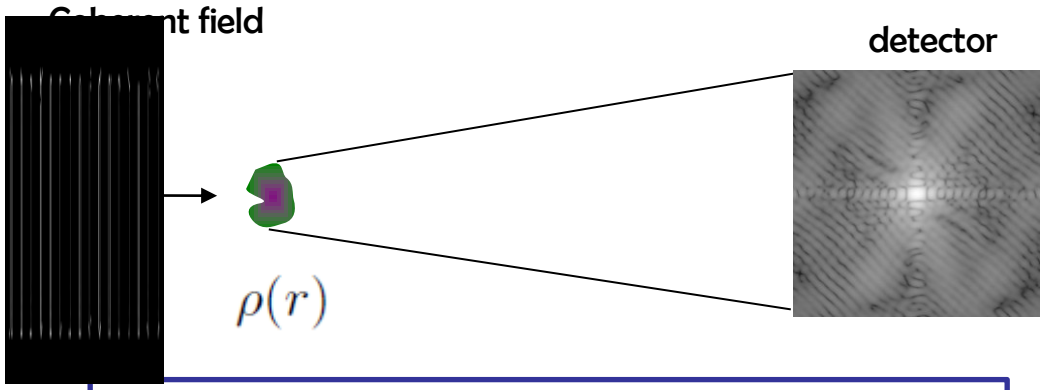

$$I(q) = |\mathcal{FT}[\rho(r)]|^2$$

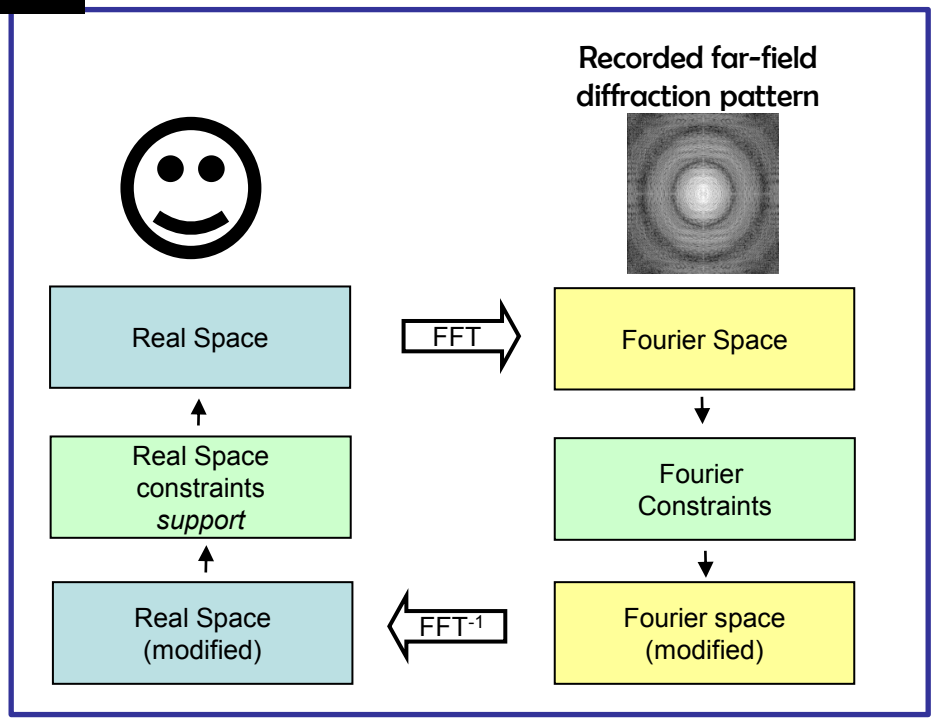

R.W. Gerchberg & W.O. Saxton, *Optik* **35**, 237 (1972)
J.R. Fienup, *Appl Opt.* **21**, 2758 (1982)

Phase retrieval algorithms cont.

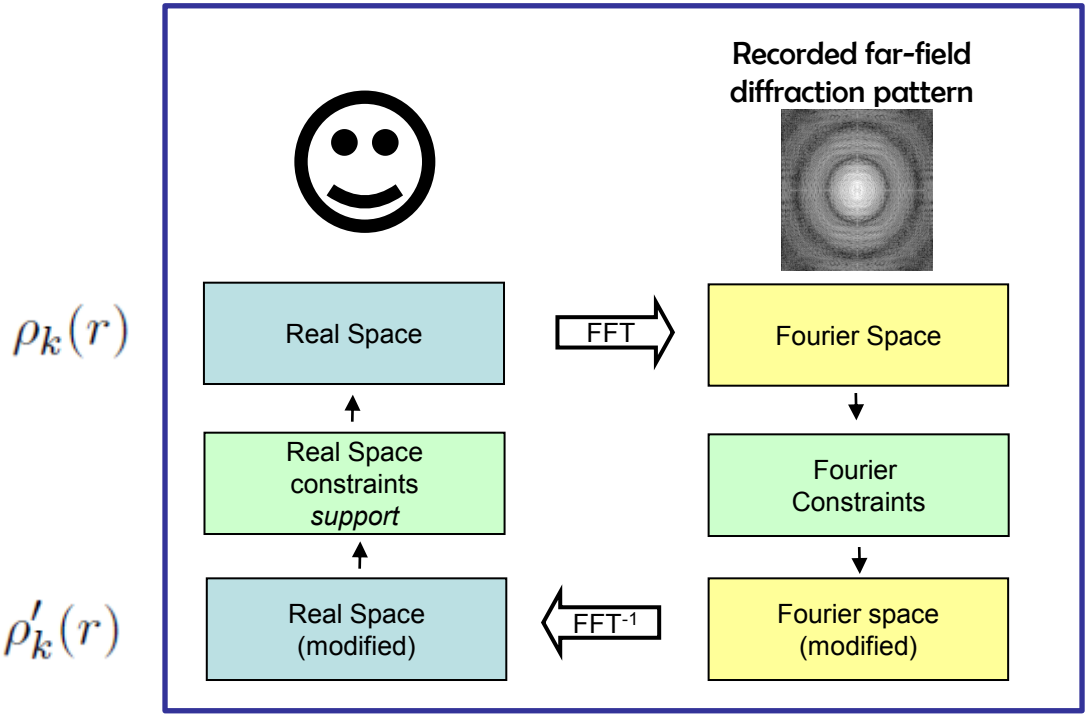

$$\rho_{k+1}(r) = \begin{cases} \rho'_k(r), & r \in S \\ \Delta(r), & r \notin S \end{cases}$$

$\Delta(r) = 0$ error reduction

$\Delta(r) = \rho_k(r) - \beta\rho'_k(r)$ HIO

$\Delta(r) = -\rho'_{k+1}(r)$ charge-flipping

S. Marchesini, Rev. Sci. Inst. 78, 011301 (2007)

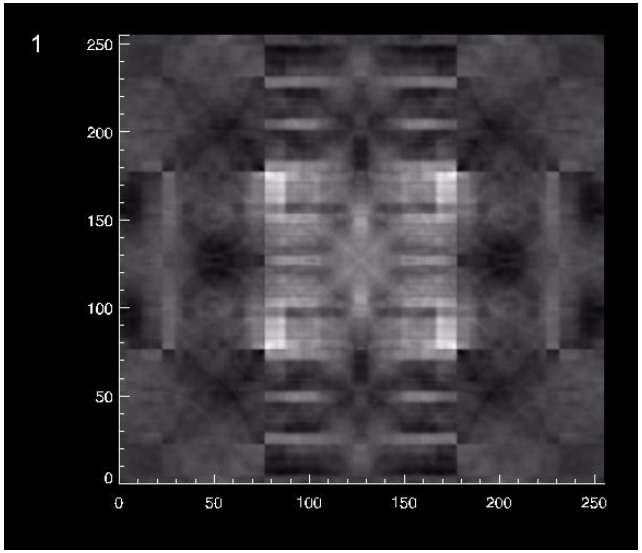
1
250
200
150
100
50
0
0
50
100
150
200
250

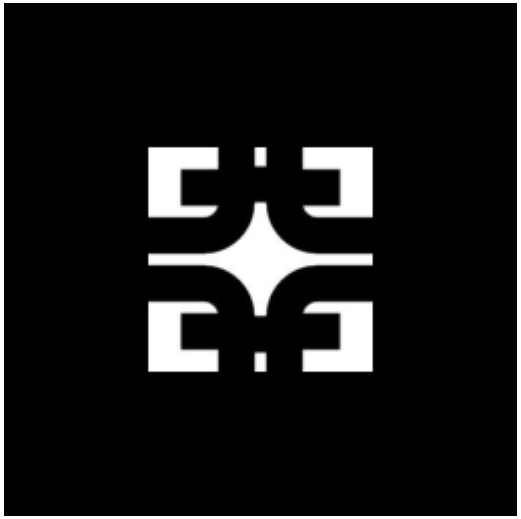

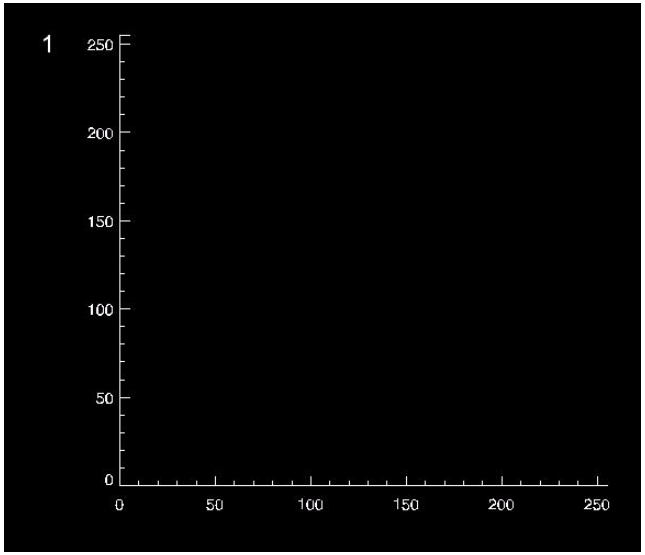
1
250
200
150
100
50
0
0
50
100
150
200
250

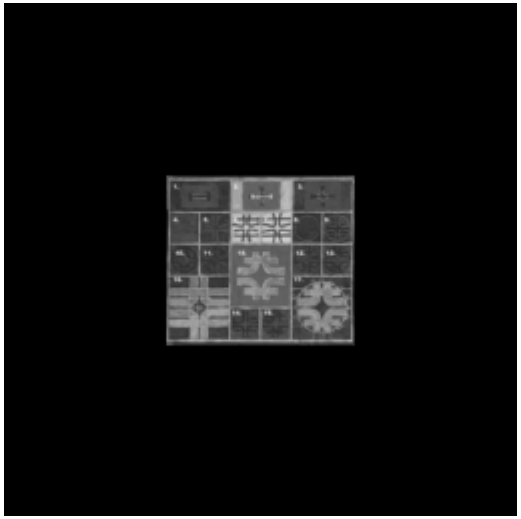

1D phase retrieval

$$\mathcal{F}[\psi(x)] \equiv \breve{\psi}(k_x) \equiv \frac{1}{\sqrt{2\pi}} \int_{-\infty}^{\infty} \psi(x) e^{-ik_x x} dx.$$

The 1D problem has in general no unique solution. Some *a priori* information on the solution is needed. Under some assumption of finite extent solution a log dispersion relation can be written

$$\mathrm{Arg}\breve{\psi}(\kappa) = -\frac{1}{\pi}\int_{-\infty}^{\infty} \frac{\log_e |\breve{\psi}(k_x)|}{k_x - \kappa} dk_x - \kappa q + \gamma + 2\sum_{j=1}^{n} \mathrm{Arg}(\kappa - \xi_j),$$

The minimal phase is the logarithmic Hilbert transform of the amplitude of the (measured) Fourier transform.

But

Ambiguities inherent to the inversion process under specific transformation:

$$\psi(x) \to e^{i\alpha}\psi(x),$$

$$\psi(x) \to \psi(x + x_0),$$

$$\psi(x) \to \psi^*(-x).$$

D. Paganin, "Coherent X-ray Optics"

Production of coherent 1D x-ray wave fields

MONASH University

Planar x-ray waveguides produce a coherent line-like focus.

μXRF@Elettra with E=7.6 keV

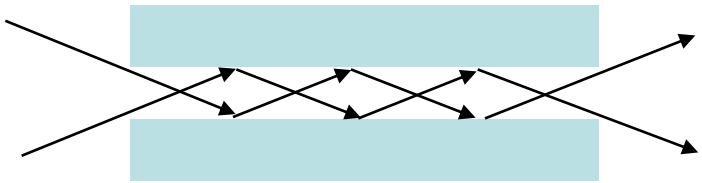

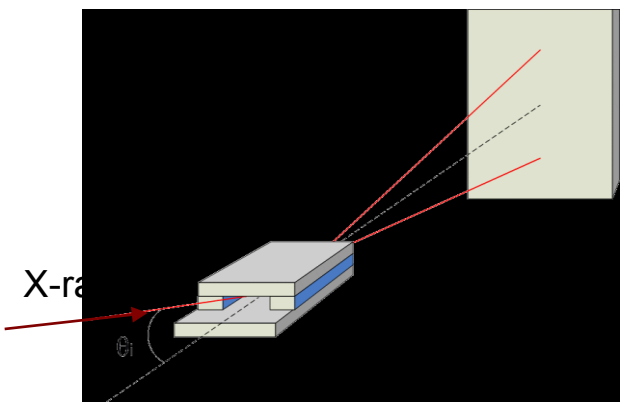

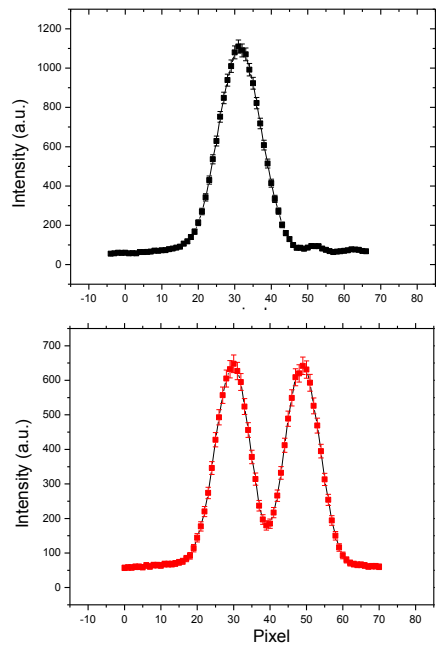

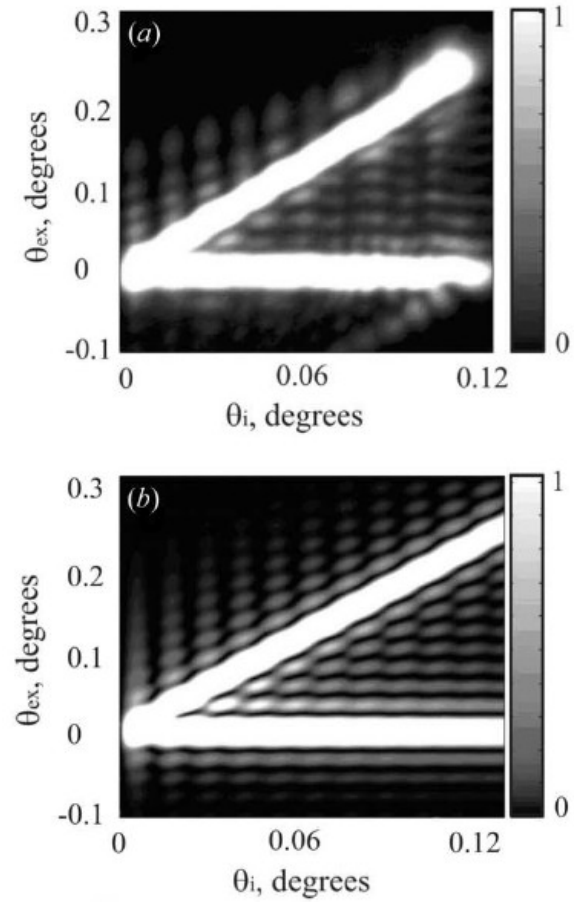

D. Pelliccia et al. *Spectroc. Acta B*, **62** 215 (2007).

I. Bukreeva et al. J. Synchrotron Rad. **17**, 61 (2010).

Correlation approach for retrieval of 1D wave fields

MONASH University

1. N independent runs of the algorithm

$$\psi^j = |\psi^j| \exp(i\phi^j),\ (j = 1, \ldots, N)$$

2. Calculate correlation between the retrieved phases of any pair of solutions:

$$c_n^{lj} = \frac{\sum_k \phi_k^l \phi_{k+n}^j}{\left(\sum_k |\phi_k^l|^2\right)^{1/2} \left(\sum_k |\phi_{k+n}^j|^2\right)^{1/2}}, \qquad \bar{c}_m^{lj} = -\frac{\sum_k \phi_k^l \phi_{N-k+m}^j}{\left(\sum_k |\phi_k^l|^2\right)^{1/2} \left(\sum_k |\phi_{N-k+m}^j|^2\right)^{1/2}}.$$

3. Choose a reference (best correlated) solution and discard the poorly correlated ones.
4. Find the shift that maximizes the correlation of the remainder solutions with the reference and apply it

$$\psi_k^j \rightarrow \begin{cases} \psi_{k+\bar{n}}^j & c_{\bar{n}}^{Jj} > \bar{c}_{\bar{m}}^{Jj} \\ \psi_{N-k+\bar{m}}^{*j} & c_{\bar{n}}^{Jj} < \bar{c}_{\bar{m}}^{Jj} \end{cases}$$

5. Minimize the error introducing a global phase

$$r(\alpha) = \sum_k |\psi_k^l - e^{i\alpha} \psi_k^j|^2$$

6. Average the results

$$\psi = \frac{1}{N_1} \sum_j \psi^j,$$

D. Pelliccia et al. *Opt. Lett*, **37** 262 (2012)

Correlation approach for retrieval of 1D wave fields

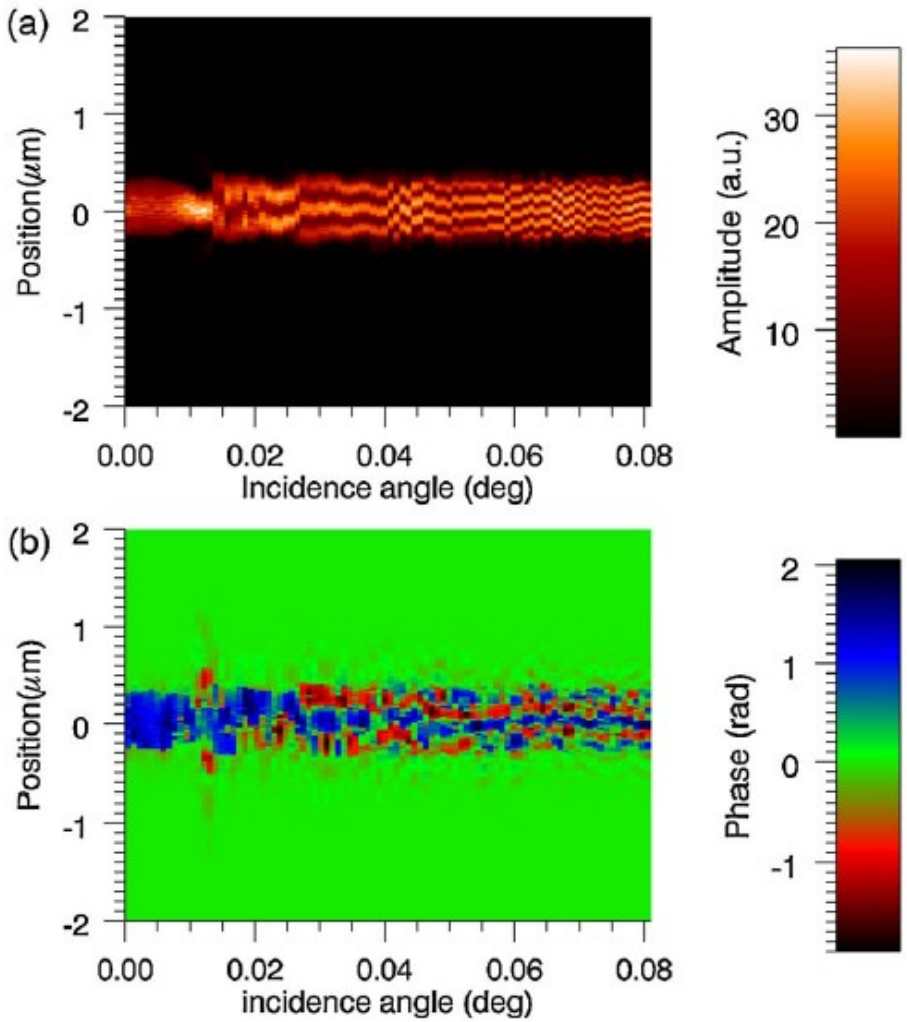

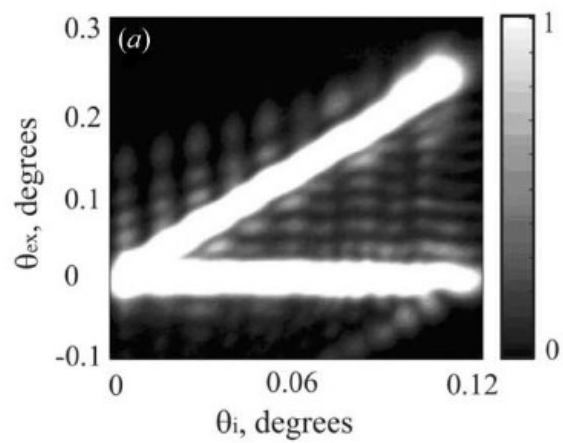

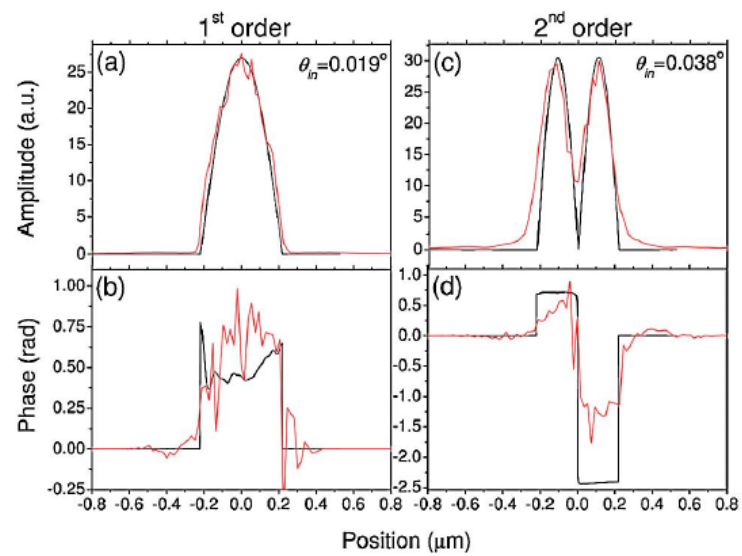

1. Development of brilliance and coherence in hard x-ray sources
2. The role of x-ray crystallography
3. The phase problem in crystallography and imaging: phase retrieval
4. **Iterative retrieval of the longitudinal charge distribution of an electron bunch**

Retrieval of longitudinal profile of electron bunch

MONASH University

The longitudinal profile of an electron bunch can be characterized by the measurement of the spectrum of the coherent transition radiation.

$$F(\omega) \propto \int \rho(t) e^{-i\omega t} \mathrm{d}t$$

Interferometric measurements give the form factor $|F(\omega)|^2$

The minimal phase can be obtained by Kramers-Kronig method, while the presence of zeros in the upper-half complex plane give an additional contribution.

First tests on the use of iterative phase retrieval:

1. Start from the minimal phase plus random contributions
2. Impose known properties of the charge distribution (i.e. real and positive)
3. Seek best convergence

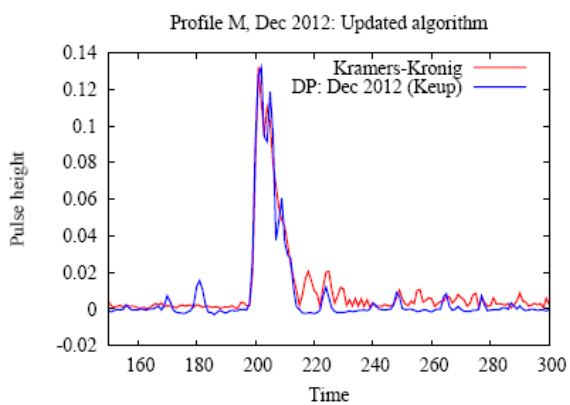

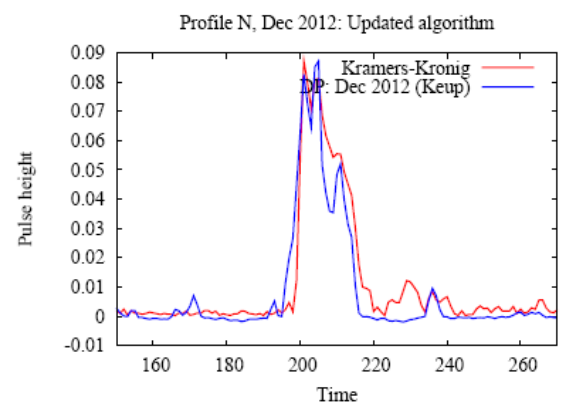

Data taken at A0 photo-injector, Fermilab with Tanaji Sen

Preliminary results...

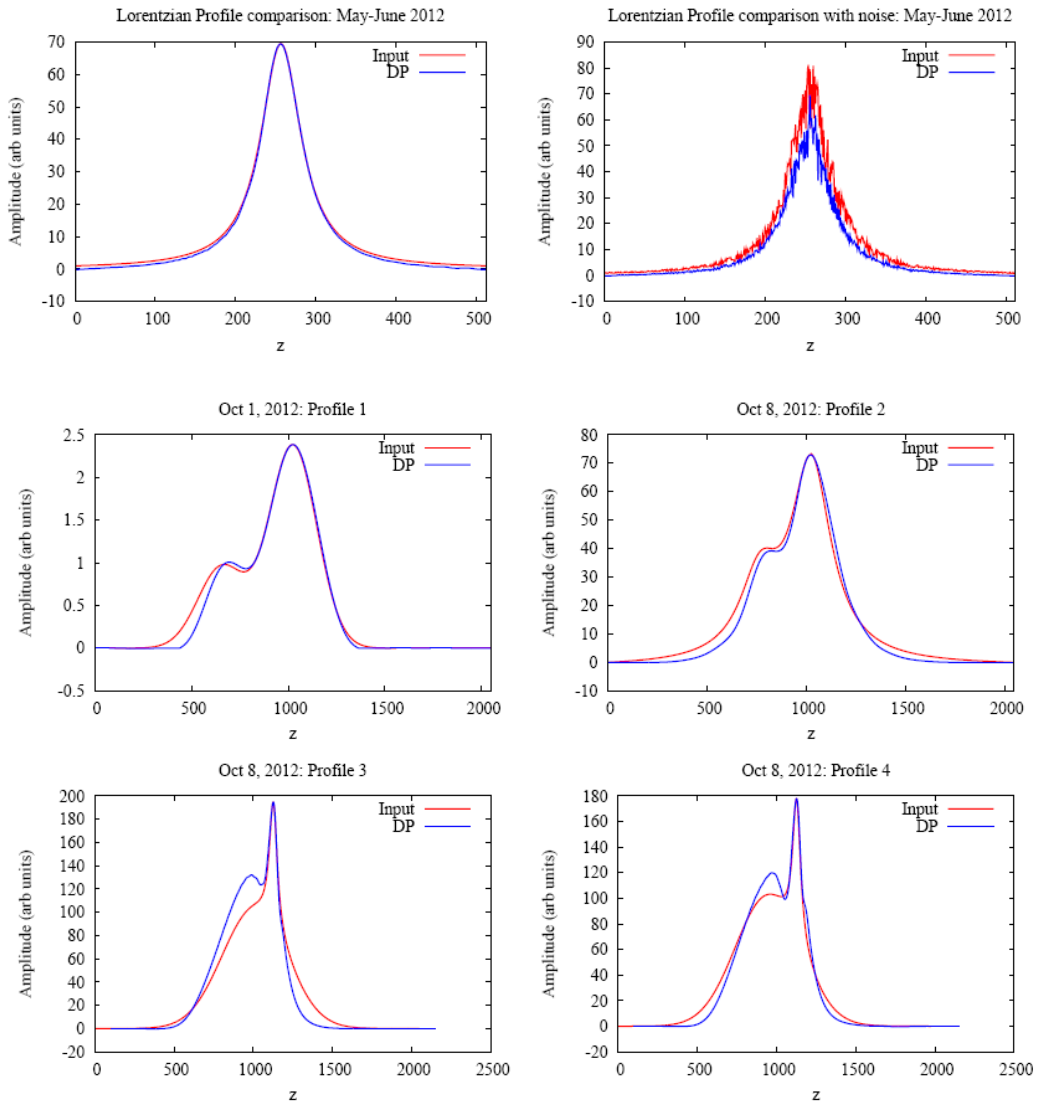

Retrieval of simulated pulse structures with Tanaji Sen

Acknowledgements

David Paganin – Monash University

Alessia Cedola – CNR Italy
Stefano Lagomarsino – CNR Italy
Inna Bukreeva - CNR Italy

Werner Jark – Elettra synchrotron

Tanaji Sen - Fermilab